

# In Vitro Electrochemical Properties of Titanium Nitride Neural Stimulating and Recording Electrodes as a Function of Film Thickness and Voltage Biasing

Justin R. Abbott, Alexandra Joshi-Imre, and Stuart F. Cogan, *Member, IEEE*

**Abstract**—Thin film titanium nitride (TiN), with a geometric surface area of  $2,000 \mu\text{m}^2$ , was deposited on planar test structures with thicknesses of 95, 185, 315, and 645 nm. Electrochemical measurements of electrochemical impedance spectroscopy (EIS), cyclic voltammetry (CV), and voltage transient (VT) were performed. We found that impedance values decreased and charge storage and charge injection capacities increased with increasing film thicknesses. Additionally, applying an anodic bias to TiN can increase the charge injection of the film to nearly double that of a non-biased film.

**Clinical Relevance**—This establishes that anodically biased TiN may provide charge injection capabilities of  $1 \text{ mC}/\text{cm}^2$  at a thickness of 645 nm.

## I. INTRODUCTION

Neural interfaces are a growing clinical treatment option for a wide variety of medical conditions. These devices, which can be implanted cortically or peripherally, serve as an electrical interface between neural tissue and computers by recording action potentials or injecting charge into neurons for stimulation [1]. One of the main failure modes of cortical implants is the encapsulation of the recording or stimulating site in fibrous tissue from chronic foreign body response. When devices are implanted, a cascading reaction begins that encases the device, pushing healthy neurons away from the electrode site [2]. One possible solution to mitigate foreign body response is to reduce the size of the electrode cross sectional area [3]. However, a consequence of the decrease of size is the reduction of the electrode geometric surface area as well. In addition to cross sectional area reduction, flexible neural interfaces are another solution to combat foreign body response encapsulation. To resolve this decrease in size, highly conductive thin films can be deposited onto the surface of the electrode sites to increase charge storage and decrease impedance.

One material successfully used in several neural interfaces is titanium nitride (TiN) [4-6]. TiN is a capacitive film that relies on its high surface roughness and porosity to have a high electrochemical to geometric surface area, effectively increasing the interface size of the electrode [7]. It has been used on large surface area electrodes like cardiac pacemakers to great effect, with high thickness TiN of about  $10 \mu\text{m}$  [4]. Recently, spinal cord stimulation devices with 200 nm thick TiN stimulating electrodes have shown chronic stability over a 16-week implantation timeline [5]. These devices utilized large,  $500 \mu\text{m}$  diameter, electrodes to drive stimulus injection capacities of  $0.15 \text{ mC}/\text{cm}^2$  during a  $200 \mu\text{s}$  pulse. Another study utilized TiN as a nerve stimulating cuff, again using

large electrodes of  $13,500 \mu\text{m}^2$  [6]. This study reported a charge injection capacity of  $0.5 \text{ mC}/\text{cm}^2$  while also using TiN with a thickness of 200 nm. While thin film TiN has been utilized as a stimulating electrode on large peripheral devices, for microelectrode arrays designed to have small feature sizes, thicker films may be needed to drive established injection limits of  $1 \text{ mC}/\text{cm}^2$  for cortical devices [8].

To our knowledge, no study has investigated the changes in surface and electrochemical characteristics of TiN with variable film thicknesses. Here, we examine how charge storage capacity, charge injection capacity, and impedance change as a function of TiN film thickness. We will also observe how surface morphology changes as observed through SEM. In prior work, TiN has been found to provide less charge injection capabilities when compared to iridium oxide, TiN and iridium oxide having charge injection capacities of  $0.87 \text{ mC}/\text{cm}^2$  and  $4.0 \text{ mC}/\text{cm}^2$ , respectively, when no biased is applied [7]. We examine the effect of anodically biasing TiN before a cathodic pulse. Biasing has been used to successfully increase the charge injection capacity in faradaic films such as iridium oxide but has not been thoroughly investigated in TiN [9].

## II. MATERIALS AND METHODS

### A. Sample Fabrication

Planar test structures were fabricated using thin film fabrication techniques in a clean room environment at the University of Texas at Dallas. 100 mm diameter test grade silicon wafers had  $3 \mu\text{m}$  of amorphous SiC deposited via plasma enhanced chemical vapor deposition (PECVD) to serve as an insulating layer. A Ti/Au/Ti metallization layer was patterned and deposited using e-beam evaporation in thicknesses of 30/300/30 nm for Ti/Au/Ti respectively. Another layer of  $3 \mu\text{m}$  thick insulating a-SiC was deposited via PECVD matching the first deposition. Electrode sites and contact pads were plasma etched out of the top layer of SiC with an SF<sub>6</sub> plasma based reactive ion etching process. Finally, TiN deposition sites were patterned onto the wafer using the same process as the metallization layer.

For the deposition of titanium nitride films, each sample was loaded into an AJA 1500 Magnetron Sputter Deposition tool, with a maximum of 1 wafer loaded per run. Before the deposition of TiN, an adhesion layer of Ti metal was sputtered onto the wafer for 4 minutes, which we later determined was approximately 30 nm thick. This adhesion metal was deposited at 4 mTorr with 50 sccm Ar gas flow and 200 W RF power. Next, 20 sccm of Ar and 1 sccm of N<sub>2</sub> was introduced to the

chamber at 40 mTorr where the plasma for TiN deposition was struck at 200 W RF power. Pressure was gradually reduced to the desired deposition pressure of 4 mTorr and 4 minutes of pre-sputtering before the shutter was opened for deposition. Deposition times of 15, 30, 60, and 120 minutes were employed. Film thickness measurements were made by scanning electron microscopy (SEM) of fracture cross-sections. Unless otherwise stated, the geometric surface area (GSA) of all electrodes is 2,000  $\mu\text{m}^2$ .

### B. Electrochemical Measurements

Electrochemical measurements were carried out using a Gamry Instruments 600 potentiostat and a Pt counter and Ag|AgCl reference electrode in a 3-electrode configuration inside a Gamry VistaShield Faraday cage. All measurements were carried out in pH balanced (pH = 7.4) and air equilibrated phosphate buffered saline (PBS) at room temperature. A total of 8 electrode sites were tested per wafer. Open circuit potential (OCP), electrochemical impedance spectroscopy (EIS), cyclic voltammetry (CV), and voltage transient (VT) were performed in that order. OCP data was collected over a period of 60 s, measuring the potential between the working and reference electrode. This potential was used as the reference point for the following EIS and CV measurements.

In EIS, the potential of the working TiN electrode was varied about OCP with a sinusoidal RMS voltage of  $\pm 10$  mV at 10 points per decade from 100 kHz to 1 Hz. We report the 1 kHz impedance as it is the most relevant for physiological recording setups.

Cyclic voltammetry data was used to calculate the total charge available for stimulation. The potential of the working TiN electrode was swept between +0.9 V to -0.9 V vs Ag|AgCl and the current response recorded. This potential range approximates the water electrolysis limits for TiN at pH 7.4. CV measurements were carried out at 50 mV/s and at 50,000 mV/s sweep rates. The 50 mV/s sweep rate was chosen to elucidate conducting pathways into the pores of the film by allowing sufficient time for transport within the pore structure of the TiN. The 50,000 mV/s provides information about reactions located near the surface of the film. Cathodal charge storage capacity ( $CSC_c$ ) was calculated by integrating the cathodic current over time during a complete CV and dividing the calculated charge by the geometric surface area as shown in Equation 1.

$$CSC_c = \frac{\int_0^t I(t) dt}{GSA} \quad (1)$$

Voltage transient measurements were used to determine charge-injection capacity using a custom-built stimulator (Sigenics, Inc. Chicago, IL) that generates a monophasic cathodal pulse with interpulse bias control to maintain charge balance. Current pulses were delivered at 50 Hz with a pulse duration of 200  $\mu\text{s}$  for the leading cathodal phase. There is a short period following the end of the cathodal phase during which the applied current is zero. The maximum negative potential excursion of the electrode is measured 12  $\mu\text{s}$  after the end of the cathodic pulse.

### III. RESULTS

Scanning electron microscopy of the surface morphology of the TiN as a function of film thick is shown in Fig. 1. The

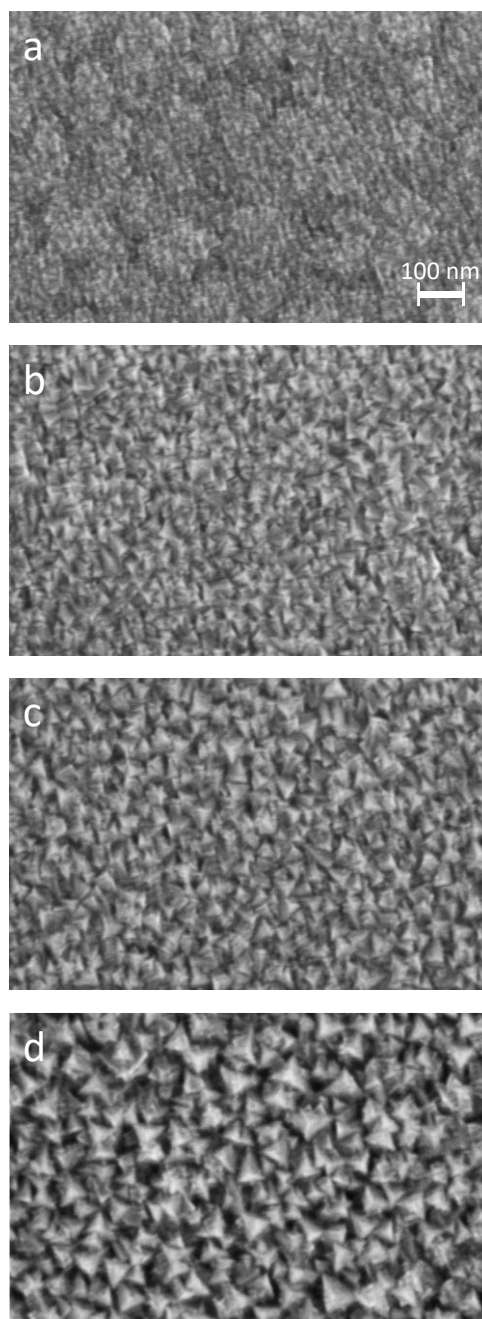


Figure 1. Film morphology revealed through SEM. Increasing deposition times lead to increased pyramidal crystal features on the surface of the film. Film thicknesses pictured are (a) 95, (b) 185, (c) 315, and (d) 645 nm. All magnifications, working distances, and voltages are the same for each image.

morphology of the film changes with increasing deposition time and thickness, with the crystal facets of the TiN becoming more pronounced as thickness increases. This growth morphology effectively increases the electrochemical surface area by increasing the depth of the columnar structure of the film. A cross section of this column structure of TiN can be seen in Fig. 2. Film thickness of TiN increased nearly linearly with deposition time, with the thickness of 95 nm, 195 nm, 315 nm, and 645 nm for 15, 30, 60, and 120-minute deposition times, respectively.

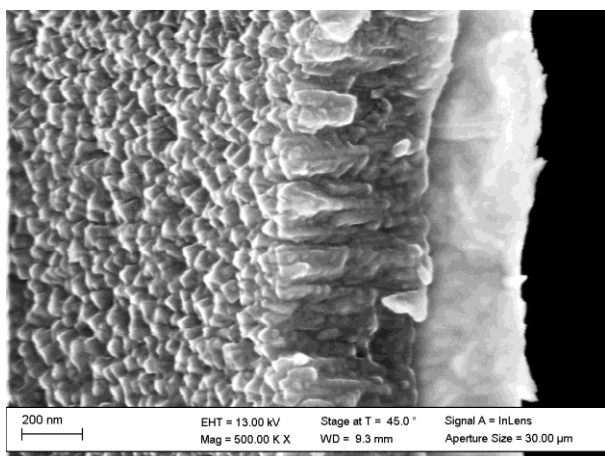


Figure 2. Cross sectional SEM of TiN showing the columnar structure and pores of the film. Pictured film is 645 nm thick.

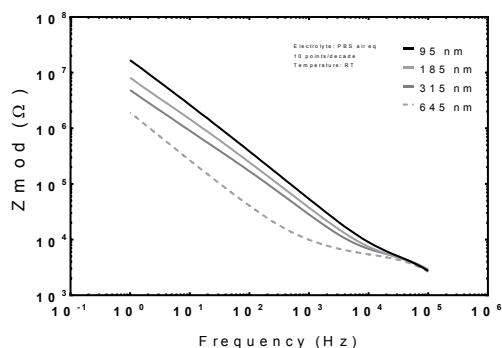


Figure 3. Representative impedance spectra showing increasing impedance values as frequency decreases and the films exhibit more capacitive behaviors. Thicker electrodes appear to have a reduced impedance compared to thinner electrodes. Measurement taken at 10 mV RMS open circuit potential vs Ag|AgCl.

The electrochemical properties of TiN also varied with film thickness, exhibiting decreasing impedance and increasing charge storage capacity as the film thickness increased (Table 1). At frequencies above 10 kHz, all TiN films exhibit a similar impedance established by the surface area of the electrodes and the electrolyte resistance. Impedance magnitudes begin to increase as the films exhibit capacitive behaviors with decreasing frequencies down to 1 Hz. Thinner films of TiN see a larger increase in impedance as this transition occurs. The average 1 kHz impedance for the 95 nm thick TiN was  $54.3 \pm 0.74$  k $\Omega$  (mean  $\pm$  S.D., N = 20, 3 depositions), which decreased to  $10.2 \pm 0.53$  k $\Omega$  for the 645 nm films as shown in the Bode plots in Fig. 3.

Cyclic Voltammetry showed that available charge storage capacity increased as film thickness increased, for both slow 50 mV/s (Fig. 4) and fast 50,000 mV/s (Fig. 5) sweep rate CVs. All CVs exhibit a capacitive shape with expected tails near the water window of  $\pm 0.9$  V. CSC<sub>c</sub> values increased as film thicknesses increased, and as expected, values were observed to be lower at higher sweep rates. At 50 mV/s sweep rates, CSC<sub>c</sub> averaged of  $2.14 \pm 0.69$  mC/cm<sup>2</sup> for the thinnest films and  $14.4 \pm 2.01$  mC/cm<sup>2</sup> for the thickest films, while at 50 V/s sweep averages of  $0.34 \pm 0.03$  mC/cm<sup>2</sup> and  $3.51 \pm 0.54$  mC/cm<sup>2</sup> for thinnest and thickest films, respectively.

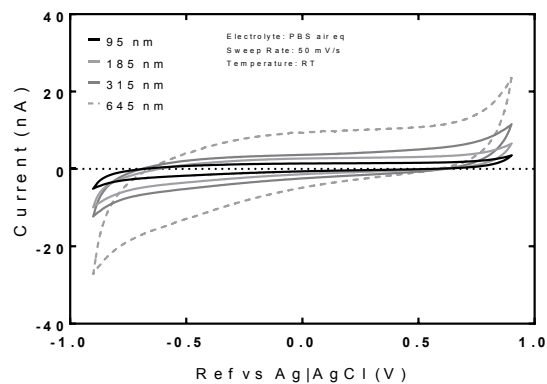


Figure 4. Representative cyclic voltammograms of increasing thicknesses of TiN. Sweep Pictured is 50 mV/s. Waveforms exhibit the expected capacitive nature of TiN.

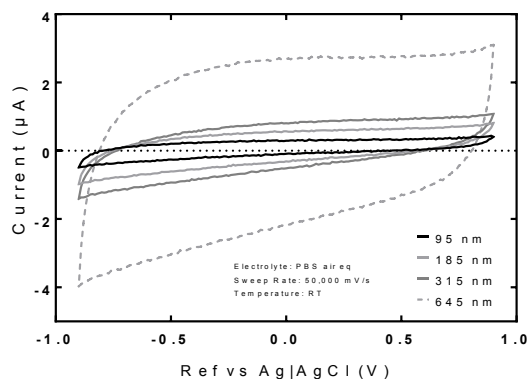


Figure 5. Representative cyclic voltammograms of increasing thicknesses of TiN. Sweep Pictured is 50 V/s. Waveforms again exhibit the expected capacitive nature of TiN. There is also a region of negative current flowing as the voltage is cycled from +0.9 to 0 V. This is most evident in the 645 nm film.

Voltage transient (Fig. 6) data showed a similar trend to that of the CV data, with thicker films delivering more charge than thinner films. 185 nm thick TiN had a maximum charge injection capacity of  $0.32 \pm 0.060$  mC/cm<sup>2</sup> while 645 nm thick films had a  $Q_{inj}$  maximum of  $0.96 \pm 0.085$  mC/cm<sup>2</sup> without any voltage bias. When applying a positive interpulse bias to these films, the maximum  $Q_{inj}$  increased by nearly 100%. With a +0.9 V bias, charge injection capacity increases to  $0.50 \pm 0.09$  and  $1.69 \pm 0.054$  mC/cm<sup>2</sup> for 185 and 645 nm thick films. Table 1 provides an overview of the TiN electrochemical properties as a function of film thickness. Charge utilization ( $Q_{inj}/CSC_c$ ) also changed with thicknesses. Without a positive interpulse bias 185 nm films exhibited a 6.1% charge utilization while biased films exhibited a 11.3% utilization. Thicker films saw a similar utilization of available charge, with 645 nm films having 6.7% and 11.7% non-biased and biased, respectively.

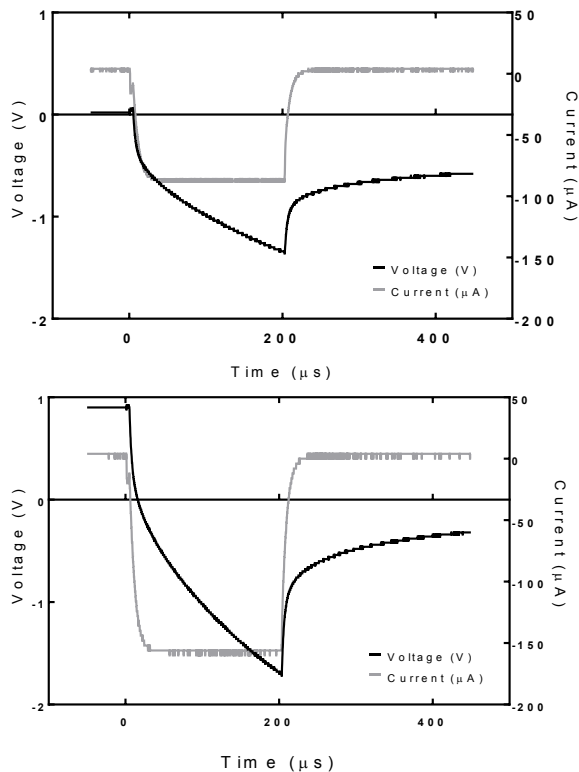


Figure 6. Voltage Transient graphs of a (top) non-biased and (bottom) +0.9 V biased TiN electrode with 645 nm thickness. Increasing the anodic bias of the film allows for more charge injection of these films.

#### IV. DISCUSSION AND CONCLUSION

Like the findings of Weiland et al. in 2002 and expanded by Maeng and Chakraborty et al. 2020, titanium nitride does not appear to match the charge injection capacities of activated or sputtered iridium oxide [8][9]. However, these films do display charge injection values near  $1 \text{ mC/cm}^2$  when biased to +0.6 and +0.9 V making them potentially useful as a neural stimulation electrode coating. Given the shapes of the 50,000 mV/s CV (Fig. 5), there is cathodic current available in the CV as the electrode is cycled from +0.9 to 0 V. This is indicative that there is charge available for biased pulsing that was not evident in the 50 mV/s CV. This area under the curve in this fast sweep CV is most notable in the 645 nm thick film and somewhat noticeable in the 345 and 185 nm thick films. This may explain why these were able to increase their charge injection capacities to a greater current injection maximum from biasing.

At the time of writing this paper, the consequences of biasing a film like TiN for chronic pulsing are not known. The current needed to sustain a positive bias must be understood to ensure that it is safe to avoid damaging neural tissue. This is especially necessary when moving from a saline environment to chronic implantation in animal cortex.

Impedance values of the thinnest 95 nm films do have 1 kHz magnitudes of electrodes that have shown the capability to record single unit action potentials in cortex. As the size of

TABLE I. ELECTROCHEMICAL PROPERTIES OF TiN DEPENDENT ON FILM THICKNESS

Film Thickness (nm)	1 kHz $ Z $ (k $\Omega$ )	CSCc at 50 mV/s (mC/cm <sup>2</sup> )	CSCc at 50 V/s (mC/cm <sup>2</sup> )	Non-biased $Q_{inj}$ (mC/cm <sup>2</sup> )	+0.6 V biased $Q_{inj}$ (mC/cm <sup>2</sup> )	+0.9 V biased $Q_{inj}$ (mC/cm <sup>2</sup> )
98	54.3	2.14	0.34	0.15	~	~
185	39.2	4.42	0.98	0.27	0.31	0.5
315	33.4	6.12	1.56	0.32	0.37	0.61
645	10.2	14.4	3.51	0.96	1.33	1.69

arrays decrease and require the use of ultra-micro or potentially nano electrodes; the impedance of TiN electrode films may require a 1 kHz impedance of less than 100 k $\Omega$  to record single unit action potentials. The characteristics of TiN electrodes smaller than the 2,000  $\mu\text{m}^2$  reported in this paper must be understood.

Thin film titanium nitride does not appear to match the in vitro charge injection capability of previously reported iridium oxide films [8][9]; however, with the application of an anodic bias prior to stimulation, titanium nitride may exceed the stimulation performance of platinum or platinum iridium alloys. Given that titanium nitride is a capacitive film and not faradaic as iridium oxide and thus less likely to generate noxious products during charge injection, there may be a benefit to using thin film titanium nitride in chronic stimulating and recording neural interfaces.

#### REFERENCES

- [1] W. M. Grill and R. F. Kirsch, "Neuroprosthetic Applications of Electrical Stimulation," *Assistive Technology*, vol. 12, no. 1, pp. 6–20, 2000.
- [2] V. S. Polikov, P. A. Tresco, and W. M. Reichert, "Response of brain tissue to chronically implanted neural electrodes," *Journal of Neuroscience Methods*, vol. 148, no. 1, pp. 1–18, 2005.
- [3] J. P. Seymour and D. R. Kipke, "Fabrication of Polymer Neural Probes with Sub-cellular Features for Reduced Tissue Encapsulation," 2006 International Conference of the IEEE Engineering in Medicine and Biology Society, 2006, pp. 4606-4609.
- [4] M. Schaldach, M. Hubmann, R. Hardt, and A. Weikl, "Pacemaker Electrodes Made of Titanium Nitride," *Biomedizinische Technik*, vol. 34, no. 7-8, pp. 185–190, 1989.
- [5] A. Garcia-Sandoval, A. Pal, A. M. Mishra, S. Sherman, A. R. Parikh, A. Joshi-Imre, D. Arreaga-Salas, G. Gutierrez-Heredia, A. C. Duran-Martinez, J. Nathan, S. M. Hosseini, J. B. Carmel, and W. Voit, "Chronic softening spinal cord stimulation arrays," *Journal of Neural Engineering*, vol. 15, no. 4, p. 045002, 2018.
- [6] M.A. González-González, A. Kanneganti, A. Joshi-Imre, et al. Thin Film Multi-Electrode Softening Cuffs for Selective Neuromodulation. *Sci Rep* 8, 16390 (2018).
- [7] S. F. Cogan, "Neural Stimulation and Recording Electrodes," *Annual Review of Biomedical Engineering*, vol. 10, no. 1, pp. 275–309, 2008.
- [8] J. D. Weiland, D. J. Anderson, and M. S. Humayun, "In vitro electrical properties for iridium oxide versus titanium nitride stimulating electrodes," *IEEE Transactions on Biomedical Engineering*, vol. 49, no. 12, pp. 1574–1579, 2002.
- [9] J. Maeng, B. Chakraborty, N. Geramifard, T. Kang, R. T. Rihani, A. Joshi-Imre, and S. F. Cogan, "High-charge-capacity sputtered iridium oxide neural stimulation electrodes deposited using water vapor as a reactive plasma constituent," *Journal of Biomedical Materials Research Part B: Applied Biomaterials*, vol. 108, no. 3, pp. 880–891, 2019.